Available online at www.CivileJournal.org

Civil Engineering Journal

Vol. 4, No. 6, June, 2018

Finite Element Analysis of Concrete Beam under Flexural Stresses Using Meso-Scale Model

Alaa H. Al-Zuhairi [a*], Ali I. Taj [a]

[a] *Department of Civil Engineering, Collage of Engineering, Baghdad University Al-Jadriha, Baghdad, Iraq.*

Received 12 April 2018; Accepted 18 June 2018

Abstract

Two dimensional meso-scale concrete modeling was used in finite element analysis of plain concrete beam subjected to bending. The plane stress 4-noded quadrilateral elements were utilized to model coarse aggregate, cement mortar. The effect of aggregate fraction distribution, and pores percent of the total area – resulting from air voids entrapped in concrete during placement on the behavior of plain concrete beam in flexural was detected. Aggregate size fractions were randomly distributed across the profile area of the beam. Extended Finite Element Method (XFEM) was employed to treat the discontinuities problems result from double phases of concrete and cracking that faced during the finite element analysis of concrete beam. Cracking was initiated at a small notch located at the middle of the bottom face of the concrete beam. The response of plain concrete beam subjected to pure bending via two point load application was detected using (XFEM) analysis of meso-scale concrete model. Assuming full bond between aggregate particles, and mortar at interfacial zone, the flexural strength of plain concrete beam is increased when aggregate particles size is increased, so that bending and shear stress were affected by void percentage and aggregate particles distribution. The maximum deflection at midspan was increased when the aggregate particles size decreases.

Keywords: Meso-Scale Modeling; Extended Finite Element; Fracture Mechanics; Concrete Flexural Strength.

1. Introduction

Concrete is a heterogeneous composite material that in general consists of cement mortar, aggregate, and pores. Its mechanical behavior is a result from the behavior of these components together at different modeling scales starting from macro, meso, to micro scale and maybe atomic and sub-atomic scale modeling. In general, most of concrete experiments and studies are in macro scales. For better understanding mechanical behavior of concrete subjected to various loading conditions a new scale studies were developed. In the last decade, a number of meso-scale models have been proposed, e.g. Grassi [1], Ren [2], Wang [4], and Lu et al. [3].

The approximation of considering concrete as a homogeneous material can be accepted when it is within the elastic range. In this stage, dissipation of energy in the form of plastic behavior and/or surface separation during micro cracking Wang [5]. As the energy is dissipated occurred concrete is no longer in the elastic range and cannot be considered as homogenous continuum, and its behavior will be governed by the sub-material of the composite concrete and a new scale of analysis is required to overcome this problem. In this study, a meso-scale analysis was conducted to a plain concrete beam subjected to flexural loading.

The modeling of concrete in meso-scale has two approaches; image based modeling and the parameterization modeling. The image-based technique is more accurate and precise method than the general numerical methods. It is a

* Corresponding author: alaalwn@coeng.uobaghdad.edu.iq

http://dx.doi.org/10.28991/cej-0309173

real reflection of the material in the meso-scale. However, it is more presently expensive and time consuming to generate the finite element model [6] Mostafavi, and [7] Jivkov. The parameterization approach comprises two methods for modeling direct and indirect. The direct method gives more flexibility in the analysis of a meso structures. It takes into account the major parameters of the multi phases material such as shape, size, gradation and distribution of the aggregate particles, interface between aggregate particles and cement mortar, and their effect on the mechanical behavior of the concrete Wang [5]. On the other hand, the indirect method dose not comprise the modeling of concrete multi phases explicitly. Furthermore, the heterogeneity of concrete may be modeled separately with a regular FE mesh Yang [8], or by using lattice modeling for the aggregate and mortar phases Leiti [9], and Schlangen [10]. In this study the direct method will be employed for the modeling and analysis.

In meso-scale structures, concrete is considered as a multi-phase material either double phase aggregate and mortar, or three-phase (mortar, aggregates, and interfaces). The complex problems of the cracking analysis of concrete was a big challenge. Many numerical models adopted for the fracture mechanic analysis of concrete such as qusai-brittle materials in the past few decades. These numerical models also tried to interpret the energy dissipation that occur during the fracture process zone. One of these models is the smeared crack method, which relate the tangent of the softening curve to the finite element size Oliver [11], Rots [12], and Bazant [13]. An alternative powerful method is the Partition of Unity Finite Element Method (PUFEM) Melenk and Babuska [14], which developed in the last decade in the form of the mesh free methods Rabczuk [15], or the Extended Finite Element Method (XFEM) Unger [16] and Monteiro [17]. Huang [18] used three point loading test for mortar specimen with different thickness. He used the XFEM for the crack propagation and failure representation in mortar numerical models. He conclude that the XFEM is able for the representation of the crack propagation and failure of mortar specimens, moreover the results show that the thickness, and the water cement ratio of test specimens affect the crack performance. Du et al. [19] used the Extended Finite Element Method for the fracture analysis of concrete under direct tension stresses in meso-scale two dimensional model, he conclude that the macroscopic analysis scales are merely depend on the distribution, size, and the shape of aggregate. It is majorly depend on the strength of the transition zone. While in the meso-scale analysis the effect of aggregate size, shape, distribution, and strength can be concluded in concrete models.

Since the fracture mechanics of concrete is important in civil and structural engineering, the goal of this study is to understand the behavior of the fracture process of concrete under flexural stresses in smaller scale (meso-scale) and by using the XFEM technique for the representation and numerical modeling of concrete cracking and propagation. A concrete prism of standard dimensions (100 × 100 × 500) mm is considered as a bi-phasic material consisting of aggregate particles and cement mortar. It will be modeled in meso-scale, and analyzed using the Method (XFEM). The analysis involves the use of the enrichment functions and techniques such as the Level Set Method (LSM) for the crack revolution and propagation representation. The beams were subjected to a two point loading case for the fracture analysis due to flexural stresses. The generation of the meso-scale model was done in stochastic system. The aggregate particles were assumed to be elliptical, while the air voids were assumed to be circular in shape. ABAQUS program was utilized for the numerical analysis of the model. The crack initiation was localized at midspan on bottom face of prism before loading is applied. Different compressive strengths were assumed for the concrete.

2. Research Methodology

2.1. Materials Properties

The properties shown in Table 1. were assumed for the materials in the meso-scale model. The aggregate-mortar interface zone was assumed to be tied i.e. the mortar is tied to the aggregate and vice versa. The shape of aggregate particles were assumed elliptic. The maximum principle stress is the maximum stress perpendicular to the crack plane near crack tip. It is used for the crack propagation and damage evolution.

Table 1. Material properties

Material	Young's Modulus, E (MPa)	Poisson's ratio, ν	Fracture Energy N-mm/mm2	Maximum Principle Stress B1, MPa	Maximum Principle Stress B2, MPa
Aggregate	75000	0.2	-	-	-
Cement mortar	25000	0.2	0.06	2.54	3.28

The assumed material properties shown in Table 1 have been adopted by López [20]. The maximum principle stresses for the crack revolution and propagation were assumed to be equal to the maximum direct tensile strength of normal plain concrete, which was proposed by the ACI [21] to be equal to $(0.43\sqrt{f_c'} - 0.71\sqrt{f_c'})$, where; f_c' is the compressive strength of concrete (in MPa). Two compressive strength of concrete model were assumed 30 and 50 MPa. The maximum principle stress can also be computed in according to the fracture toughness principles. Callister [22], and Bazant [23] proposed a critical stress that required for crack propagation as shown in Equation 1.

$$\sigma_c = \left(\frac{2E\gamma_s}{\pi a}\right)^{\frac{1}{2}} \quad (1)$$

Where;

σc: critical stress required for the crack propagation (MPa).
a: the initial crack length in meters, which assumed to be 4 mm at midspan on bottom face of beam.
E: the modulus of elasticity of concrete (MPa).
γs: the specific surface energy (N-mm/mm^2).

2.2. Size Distribution of Aggregate Fractions and Pores

In this study, the coarse aggregate was modeled as individual particles floating randomly into cement mortar. Aggregate particles generation will start from minimum size of 4.75 mm to a maximum size of 25 mm. Three ranges of particle gradation were involved in this study to show the effect of the different sizes of the coarse aggregate particles on the behavior of the concrete prism in flexural. Table 2 illustrate the percentage passing of coarse aggregate particles. Figure 1 shows the grading of coarse aggregate that used in concrete mixes used in modeling process. The solid line in this figure represent the limit of ASTM [24] coarse aggregate of a nominal size (4.75-19).

Table 2. Particle size distribution of coarse aggregate used in analysis of concrete prism

Sieve opening, (mm)	Concrete Mix No.								
	M 1			M 2			M 3		
	Percentage passing, %	Equivalent particle size, (mm)	Mass percentage, %	Percentage passing, %	Equivalent particle size, (mm)	Mass percentage, %	Percentage passing, %	Equivalent particle size, (mm)	Mass percentage, %
25	100	18.22	10	100	18.22	10	100	18.22	10
19	90	6.95	70	90	8.40	60	90	10.00	50
9.5	20	5.50	10	30	5.50	20	40	5.50	30
4.75	10			10			10		

Pores representing air voids were modeled as circular shapes of constant size diameter of 2 mm. Air voids percentage was taken 2%, for the three concrete mixes.

2.3. Generation of Aggregate Particles and Air Voids

Pores and aggregate particles at each gradation fraction were randomly distributed through the side plane area of concrete prism. This were done through utilizing EXCLE Sheets for the calculating processes. The location of the center of ellipse and the orientation of each particle were defined randomly, and the diameter of each particle was selected with in the aggregate grading of each segment.

After placing the aggregate particle, the position of aggregate particles were reselected manually using ABAQUS graphical user interface. So the following conditions were checked: (a) all the aggregate particles are inside the concrete area, (b) Overlapping and intersection between aggregate particles was excluded, (c) aggregate particles were separated by a minimum distance (0-1) mm, (d) and covered by cement mortar of 2.5 mm at the edges of concrete beam. The same procedure was used for the generation of the pores inside concrete beam. The diameter of the air voids was assumed to be 4 mm. Shahbazi [25] stated a flow chart for the generation of the meso-scale model of concrete with rounded or crushed aggregate.

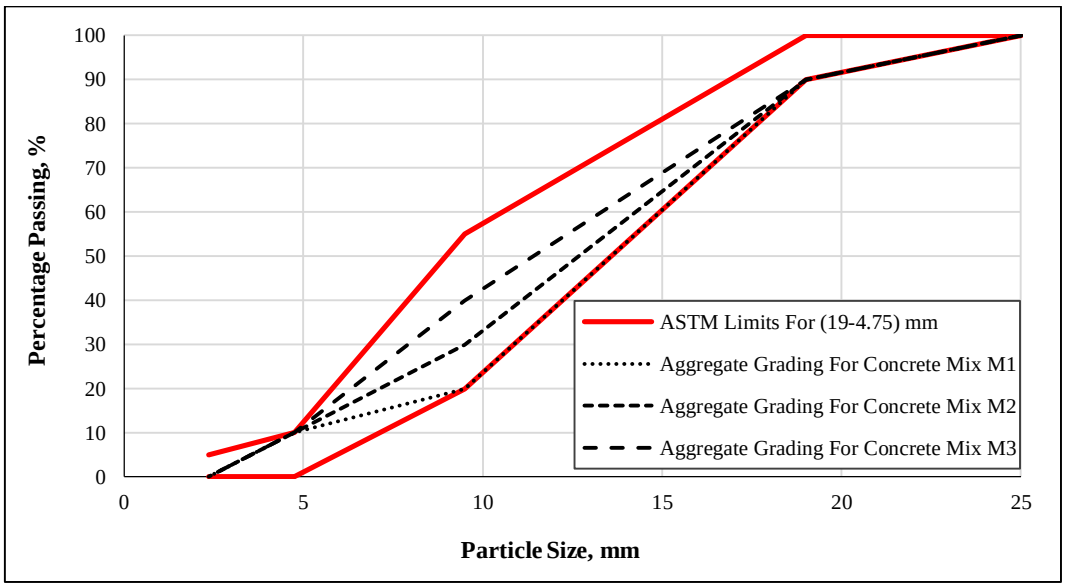

Figure 1. Grain size distribution of coarse aggregate for concrete mixes and ASTM C33 standard limits

3. Numerical Model

A plain concrete simply supported beam was used to illustrate the effect of different aggregate grading on the bending strength, shear strength, and the maximum deflection of the beam when it is subjected to two point loading. The model was constructed to be analyzed as two dimensional plan stress problem, with 500 mm span, 100 mm width, and 100 mm height. A notch of 4 mm depth was located at the center of the span on the bottom face of the beam to initiate crack (see Figure 2).

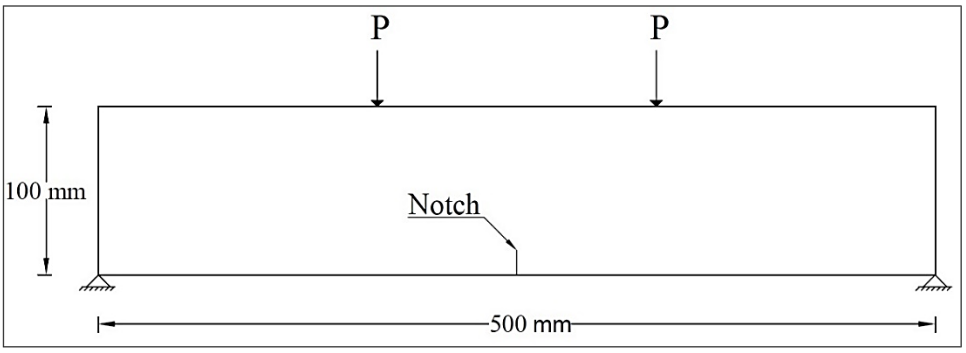

Figure 2. Concrete prism model dimensions, loading, and boundary conditions

4. Meshing and Extended Finite Element Method

The discontinuity issue in practice can be found in cracks, shear bands, and many other forms in structural problems. Discontinuity can be classified into strong and weak discontinuity, which represent respectively the cracks and the interfaces between two different materials in structural concepts Khoei [26]. The discontinuity that occurs in a concrete model is difficult to be analyzed with the conventional Finite Element Method (FEM). In order to have a better solution of the problem a suitable technique is necessary. One of the latest techniques used to solve the discontinuity problems is the Extended Finite Element Method (XFEM), Asferg [27]. The major concept of this method is the addition of the enrichment functions to the standard finite element analysis solution. It is based on the multiplication of the enrichment function by the nodal shape function. The enrichment technique could be solved on a region of the general domain by only enriching the nodes in that region. The final finite element approximation with the enrichment functions can be shown in Equations (2) and (3) shown below Khoei [26]:

$$u(x) = \sum_{i=1}^{N} N_i(x)\bar{u}_i + enrichment\ terms \tag{2}$$

$$u(x) = \sum_{i=1}^{N} N_i(x)\bar{u}_i + \sum_{i=1}^{N} \bar{N}_i(x)\left(\sum_{j=1}^{M} p_j(x)\,\bar{a}_{ij}\right) \tag{3}$$

Where;

$\bar{u}_i$: the degree of freedom of the standard interpolation

$N_i(x)$: the shape function of the standard interpolation

$\bar{a}_{ij}$: the degree of freedom of the enriched part related to the basis of $p_j(x)$

M: the number of enrichment functions for the node i

$\bar{N}_i(x)$: denoting the new set of shape functions for the enrichment region

Element were used for the analysis with XFEM. The element type in ABAQUS was specified by using the mesh controls preference. Elements size were set to 2.5 mm on the edge of the model by using the seed edges preference in ABAQUS. Crack notch located on the bottom face at midspan of the prism, with a length of 4 mm. Figure 3 shows the concrete prism models with finite element meshing for the different mixtures as shown in Table 2.

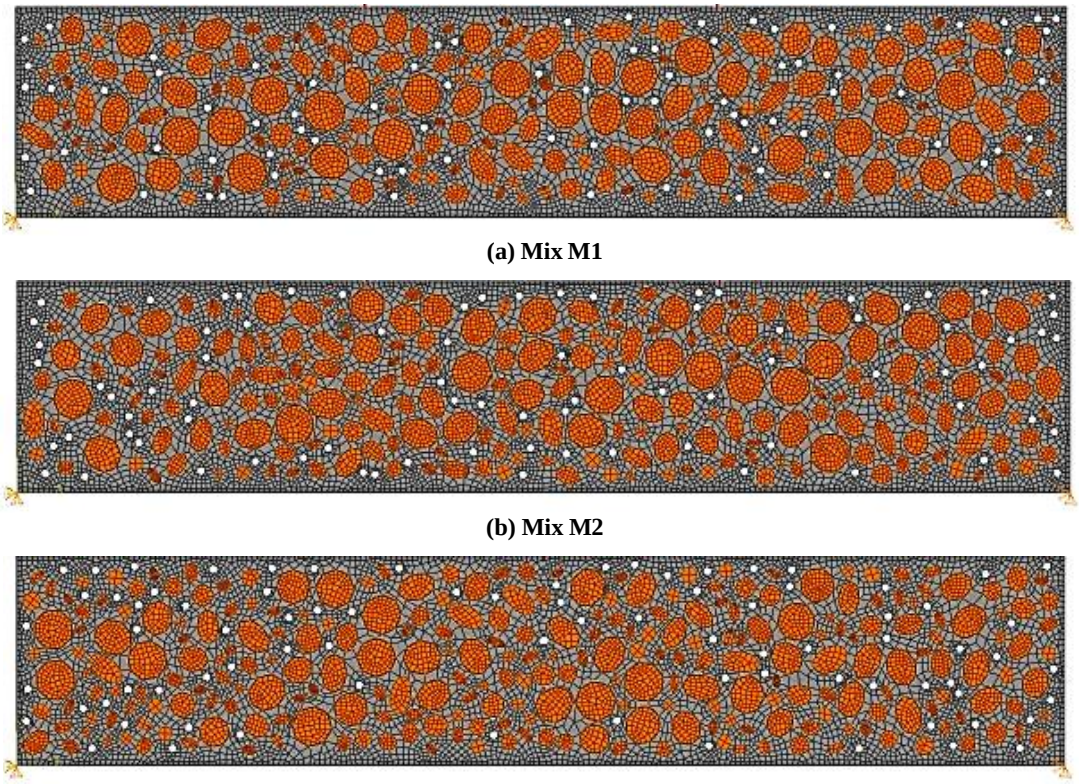

(a) Mix M1

(b) Mix M2

(c) Mix M3

Figure 3. Meso-scale FE mesh of concrete prism with different coarse aggregate percentages and 2% air voids

5. Enrichment Functions

The XFEM depends on the Partition of Unity (PU) technique for the solution of the discontinuities problems. The PU technique comprises the addition of the enrichment functions to the convenient solution as was illustrated in Equation 2. Different enrichment functions are available different applications according to the purpose they used for. For strong discontinuities such as crack the Heaviside enrichment function H(x) is commonly used. İt was first introduced by Moe's [13].

Consider a crack domain Ω with crack interface that divide the domain Ω into two parts, Ω+, and Ω-. The Heaviside enrichment function can take two values (0) for the negative part of the domain, and (1) for positive part of the domain, as can be shown in Equation 4:

$$H(x) = \begin{cases} 0 & x \in \Omega^- \\ 1 & x \in \Omega^+ \end{cases} \quad (4)$$

Another technique used for the crack surface and crack tip geometry tracking is the Level Set Method (LSM) which was introduced by Osher [28]. The main concept of this technique is the use of level set function such that the discontinuities interface for example a crack interface is represented as a zero level set function. As illustrated Equation 5 (Osher [28], and Sukumar [29]).

$$\varphi(x,t) = \pm^{min}_{x_\Gamma \in \Gamma(t)} \|x - x_\Gamma\| \quad (5)$$

Where;

Γ is the discontinuity interface, t is the applied loads on the domain Ω, and x_Γ is a point on the discontinuity interface, as shown in Figure 4.

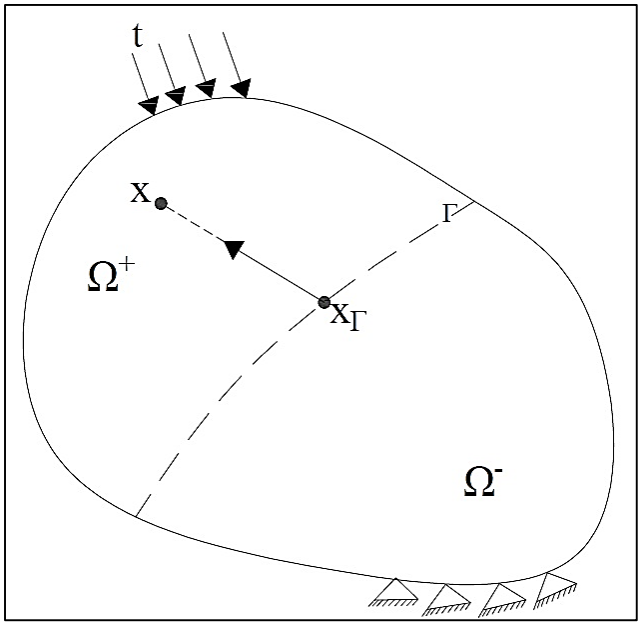

Figure 4. Problem with strong discontinuity

6. Crack Initiation Criteria

In the Extended Finite Element Method analysis it is very important to specify the crack initiation criteria. İt can be satisfied by the maximum hoop stress and the principle stress criteria introduced by Erdogan [8]. In this study, the maximum principle stress was adopted for the crack initiation and evolution as shown in material properties (section 2).

The crack initiation process start with the decreasing of the cohesive strength of the material at the enriched elements. The decreasing in the cohesive strength start when the applied tensile stresses are more than the maximum principle stress of the material at integration point, and a discontinuity in the element is introduced. The maximum principle stress is assumed to be perpendicular to the direction of the crack propagation path. In this study, the FE mesh was constructed using quadrilateral two dimensional elements. When the crack initiate a two dimensional triangular elements was introduced to divide the original quadrilateral elements. This important to note that in the XFEM, cracks cannot be intersect, coalesce, or branch.

In the fracture zone the cohesive forces is existed on the crack tip during the fracture process. These forces are acting on the both sides of the crack surfaces. The intensity of the cohesive forces depend on either the fracture energy of the material or the crack opening displacement.

7. Analysis Results and Discussion

The effect of variation of grain size percentage on the behavior of the concrete prism subjected to pure bending via two–point load application was studied. The studied behavior compromised bending stress distribution along prism axis, deflection curve, and shear stress distribution across the prism depth.

Figure 5 shows the bending stress distribution for the concrete models of compressive strength of 30 MPa, as can be seen the stress distribution near and around the crack tip is approaching to zero. When the crack propagate into the material, the zero stress region grows as shown in Figure 5 (a) for Mix M1 and the tension region is decreased. Moreover, the stress magnitudes are increased in some aggregate particles, this is due to the high strength of the aggregate. In spite

of the effect of the aggregate particles on the distribution of the stresses inside the concrete medium, the general distribution of the stresses is approximately the same when the material is homogenous

Figure 6 shows the distribution of normal stress at the bottom fiber of concrete prism result from bending. As can be seen the bending stress is falling to zero at the center of the prism span. This can be attributed to the development and propagation of the crack that initiated at the center of the span, already, which consequently made a strong discontinuity in the finite element domain that result in a plastic hinge. The bending stress curve is generally rough one, due to the non-homogeneity of the concrete. On the other hand, the presence of air voids near the bottom fiber line causes stress concentration problems as can be seen in Figure 6(a). The concrete prisms which are made from Mix M1 and Mix M2 exhibit almost the same maximum tensile bending stress of 3.8 MPa, while the third one that is made from Mix M3 was stressed by a greater maximum tensile bending stress than the other two prisms by approximately 15%. This may lead to think that the maximum flexural strength can be obtained when the percentage of the coarse aggregate is approaching the average value of grading limits that is shown in Figure 1.

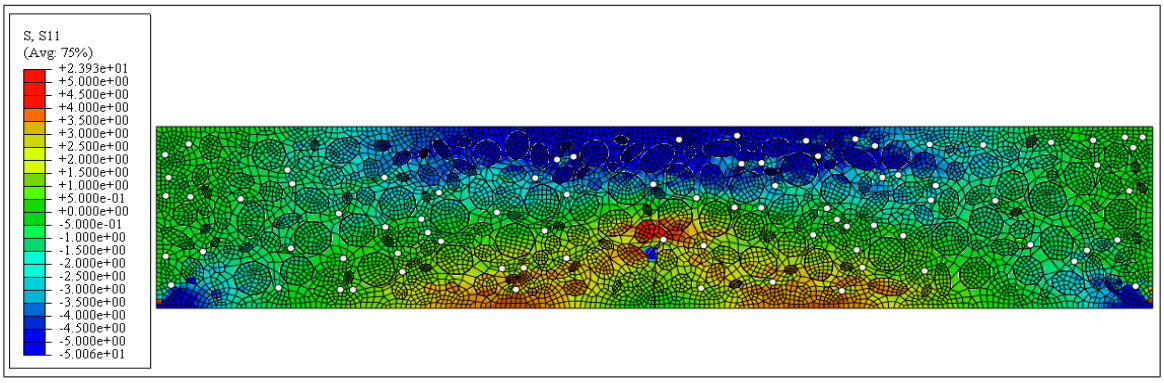

(a) Mix M1

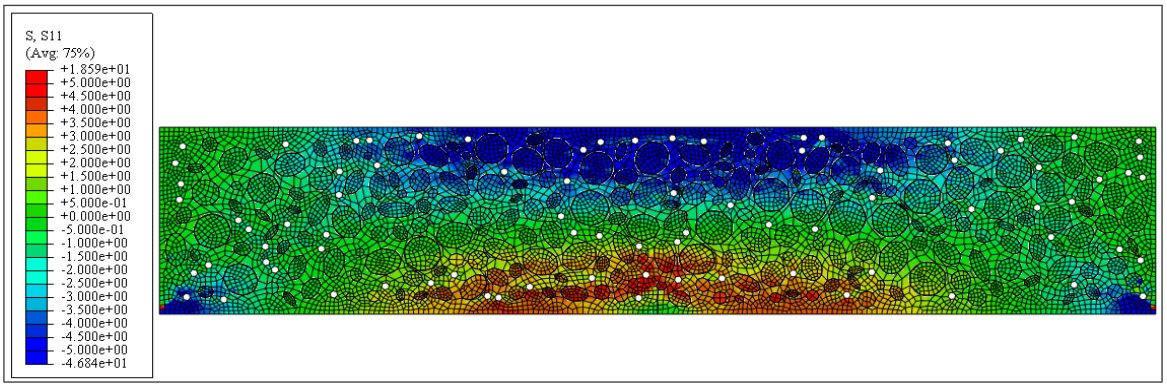

(b) Mix M2

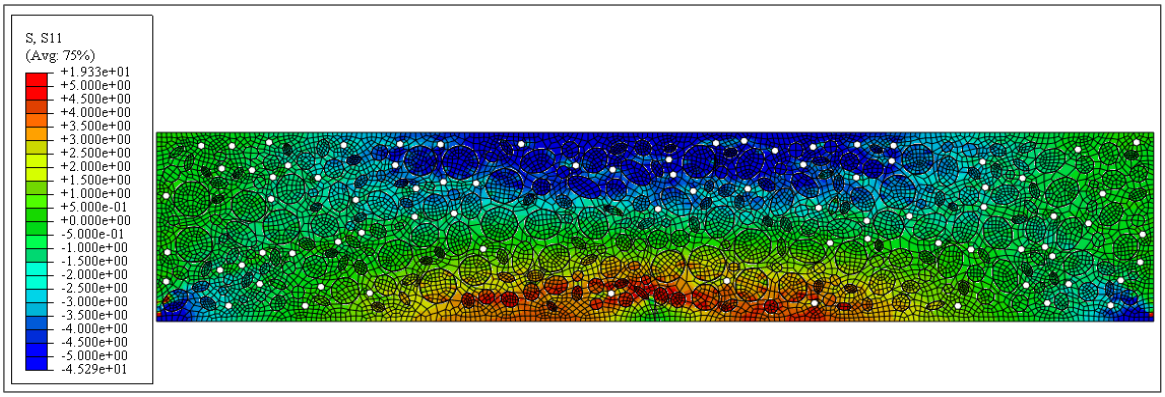

(c) Mix M3

Figure 5. Bending stress distribution at the ultimate load state

Figure 6 Shows that the maximum bending stress, which occur near crack initiation zone, is affected by the tensile strength of cement mortar. It is increased when the tensile strength increased. The increase in bending stress at crack initiation is about 28 % for Mix M2 and M3 and is about 25 % for Mix M1, which indicate that the crack initiation of

concrete is proportional to the tensile strength of the concrete. However, when the maximum size of aggregate is decreased the maximum bending stress magnitude is increased at the same applied load as shown in Figure 6.(a) for Mix M1. The difference of the maximum bending stress at last load increment for Mix M1 with different tensile strength is about 11%. This may be due to the increased homogeneity of the concrete when aggregate particles size is decreased.

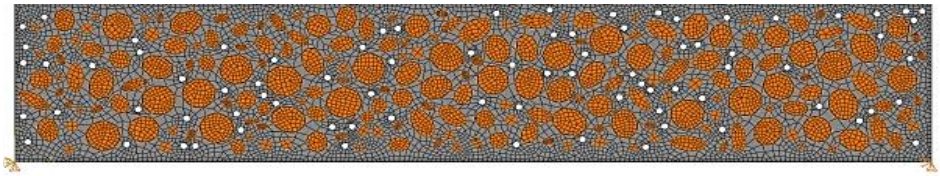

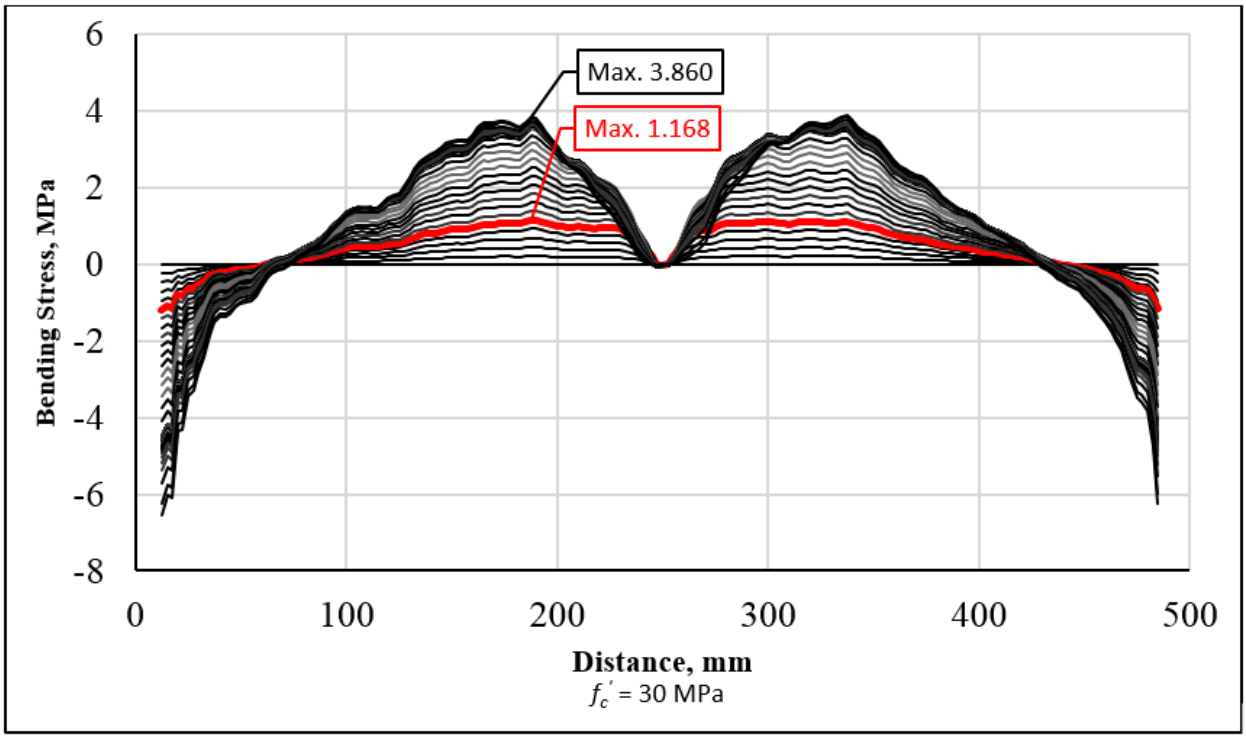

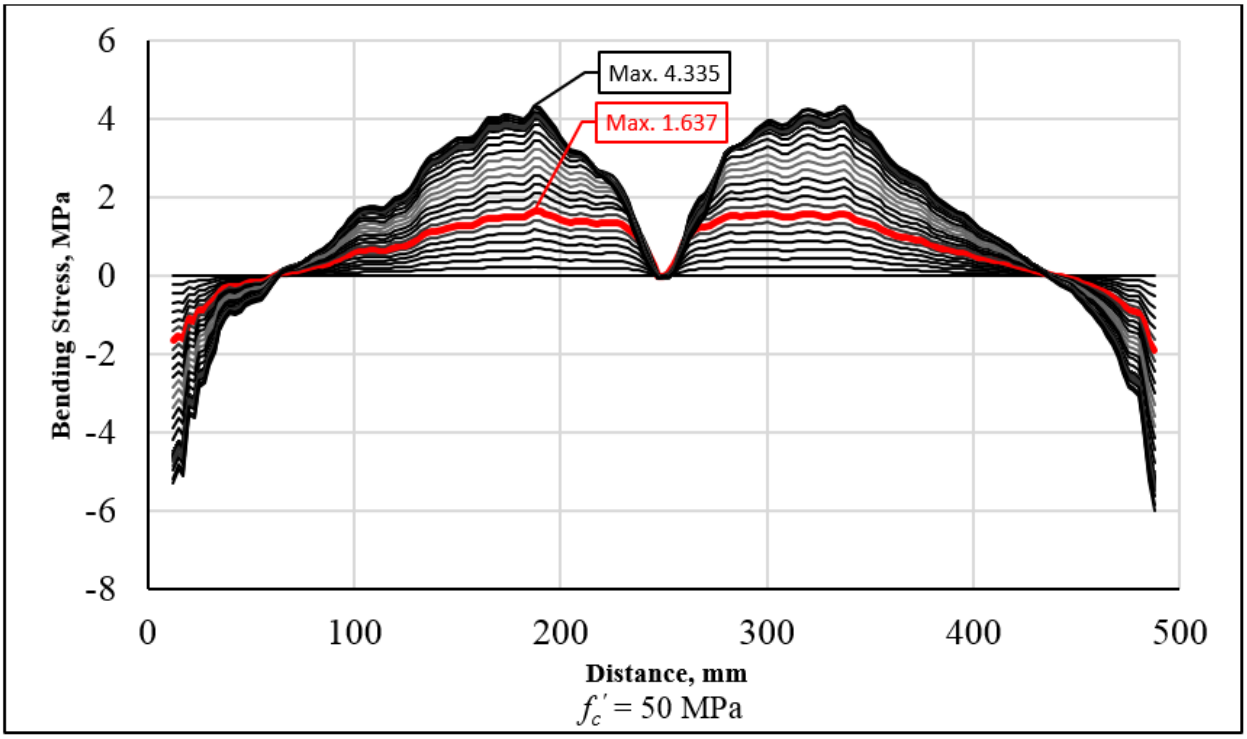

(a) Mix M1

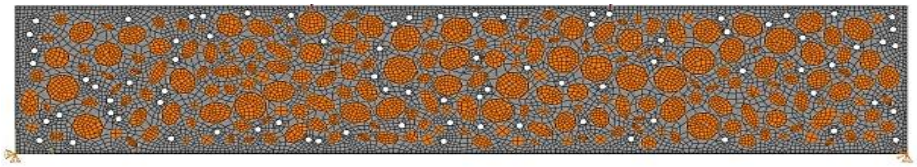

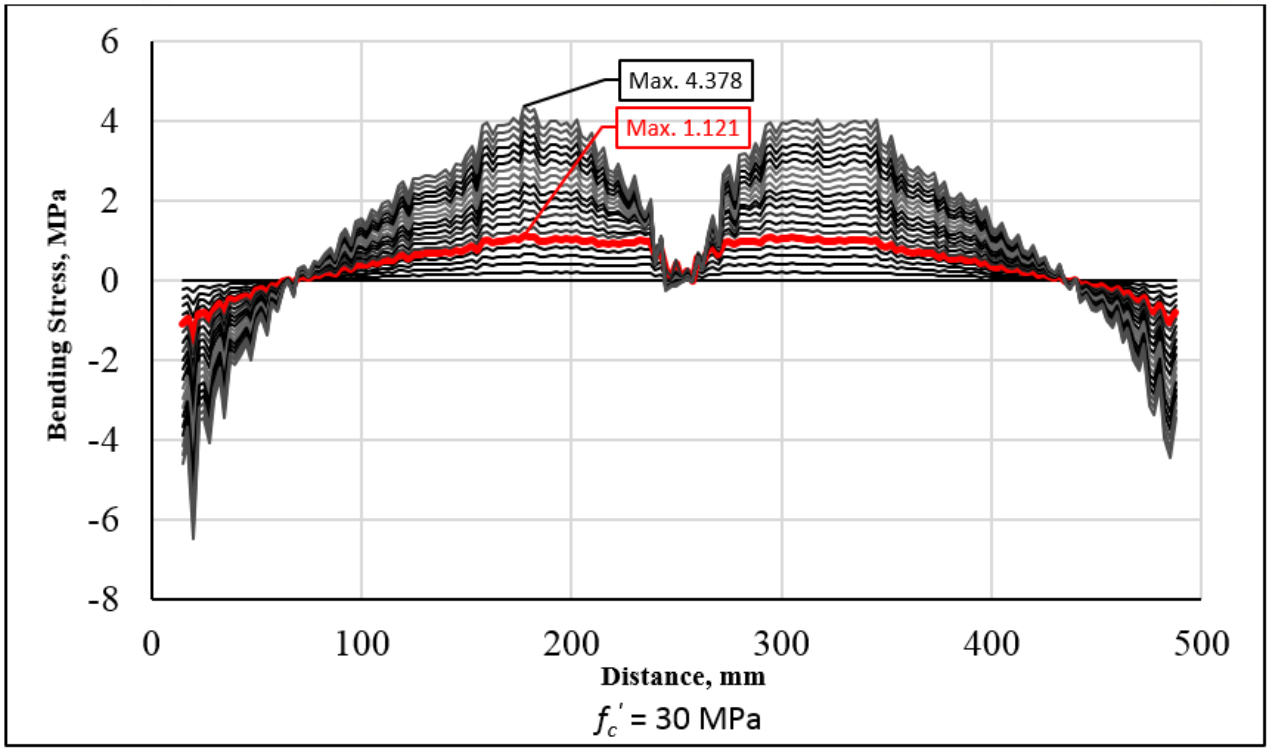
Max. 4.378
Max. 1.121
Bending Stress, MPa
Distance, mm
f_c' = 30 MPa

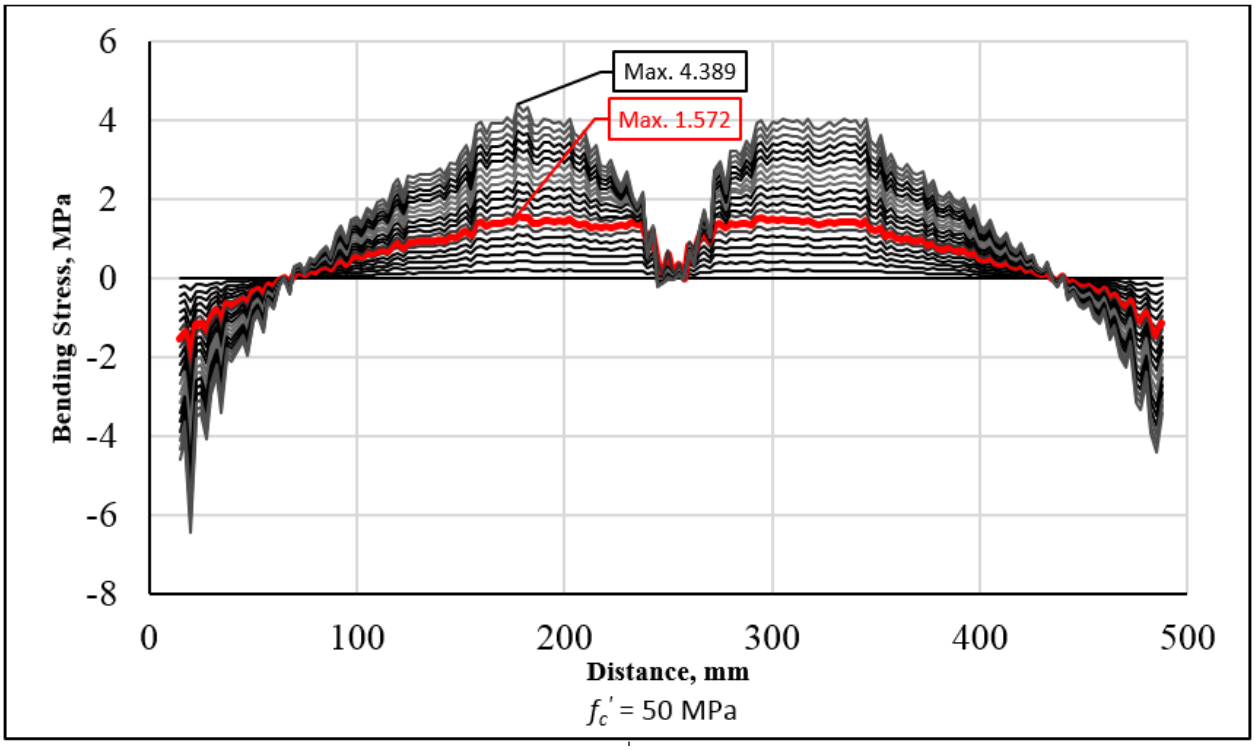
Max. 4.389
Max. 1.572
Bending Stress, MPa
Distance, mm
f_c' = 50 MPa

(b) Mix M2

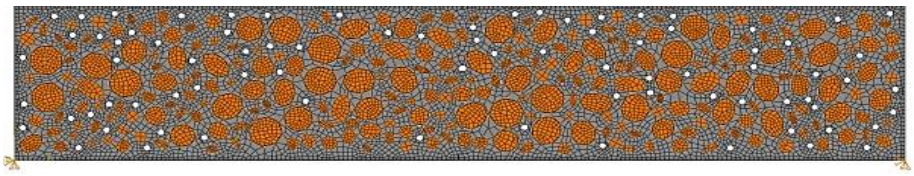

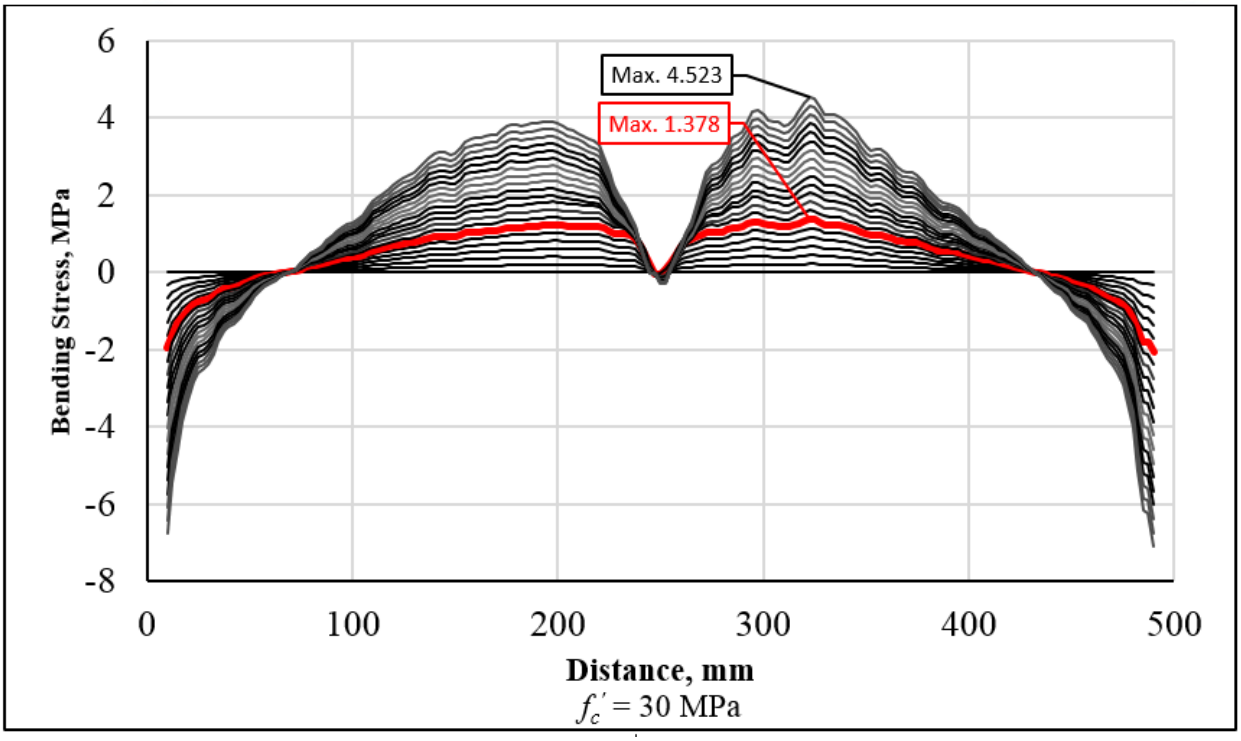

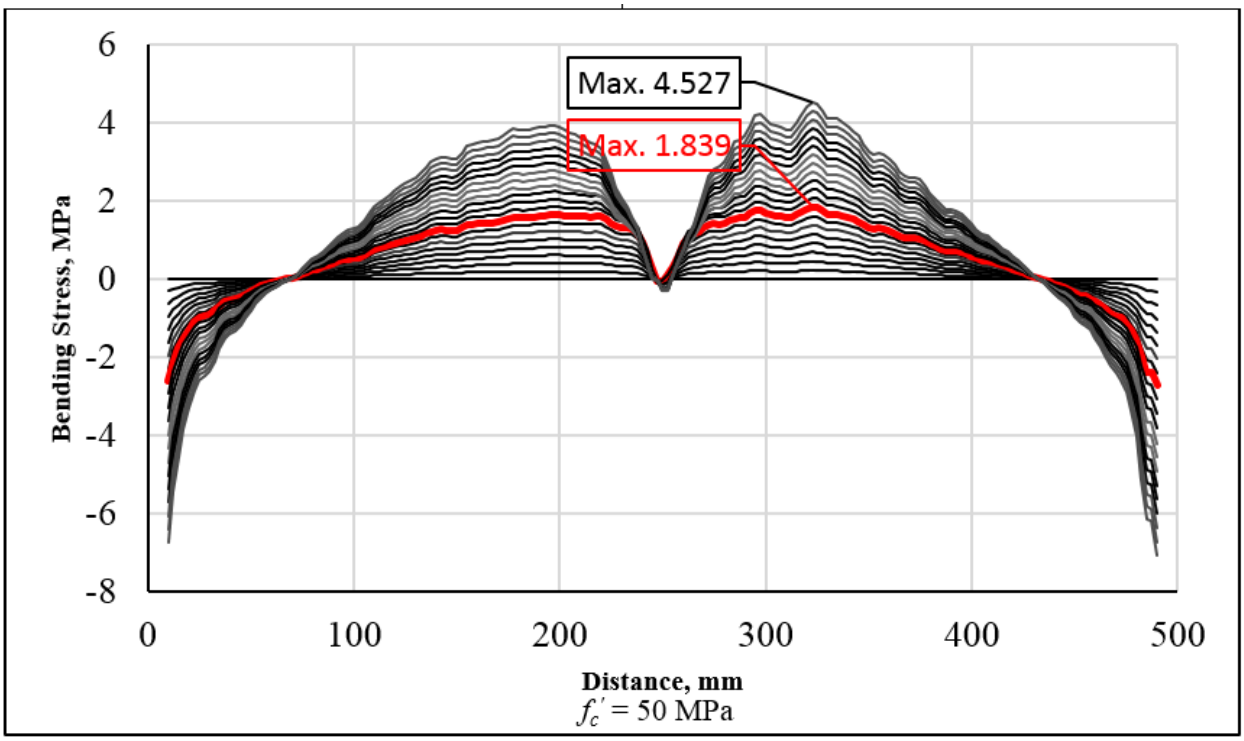

(c) Mix M3

Figure 6. Effect of variation of coarse aggregate percentage on the flexural stress of the concrete prism at crack initiation and in the last loading increment

Figure 7 shows the deflection curves for the three concrete prism models. The maximum mid span deflection (0.161 mm) occurred in the concrete prism made from Mix M1 while the minimum mid span deflection (0.127 mm) was found in prism that is made from Mix M3. The difference between the minimum and maximum deflection is about 21%.

The decrease in mid span deflection of prism made from Mix M3 may be attributed to the same cause of increase in tensile flexural stress. For f_c' = 50 MPa, the maximum deflection value is increased, however the maximum difference occurred in Mix M1, which is increased by 28 % from the same mix with f_c' = 30 MPa. While at the last load increments the maximum deflection value is decreased when the compressive strength is increased by 11 % for Mix M1 and 4.5 % for Mix M2 and M3, which indicate that increasing the tensile strength of the concrete decrease the deflection values, and maximum decreasing occurs when the aggregate particles size is decreased too.

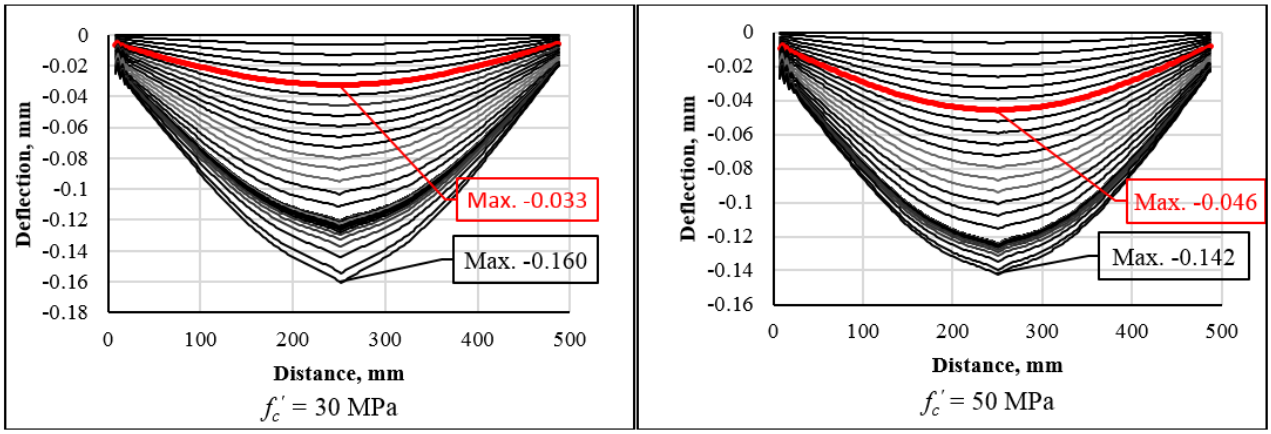

(d) Mix M1

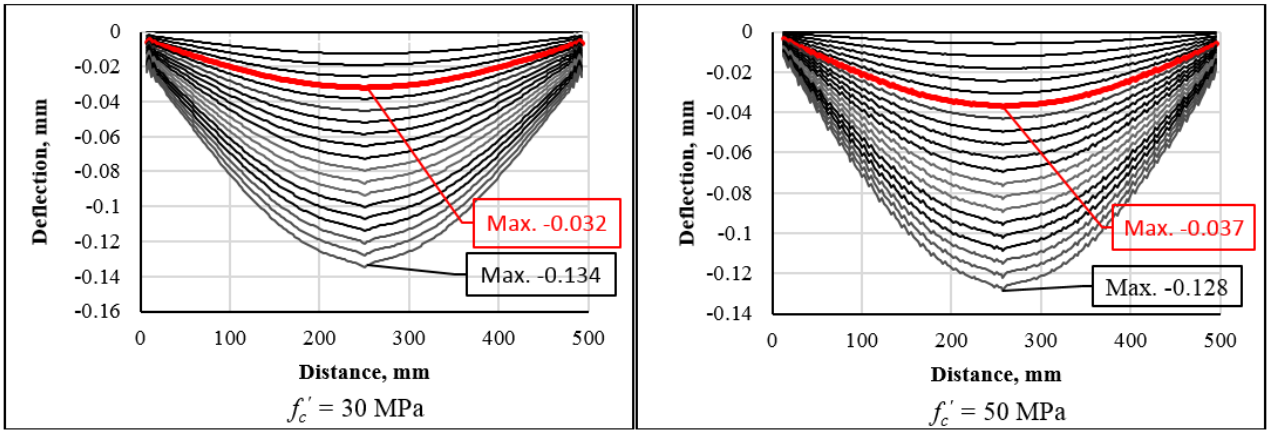

(e) Mix M2

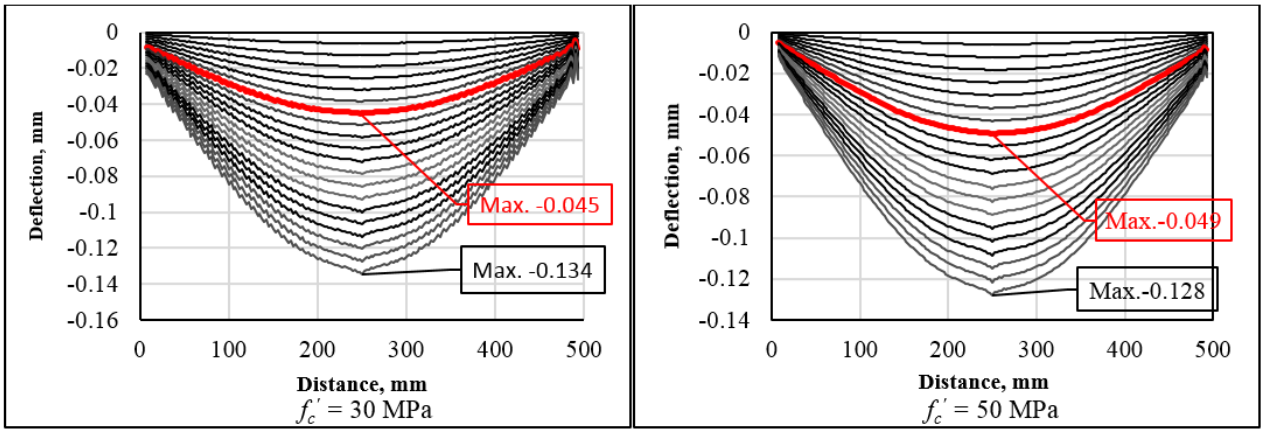

(f) Mix M3

Figure 7. Effect of variation of coarse aggregate percentages on the maximum deflection of the concrete prism model at crack initiation and in the last loading increment.

Shear stress distribution across the entire depth of prism models at a section 84 mm apart from the support. The curves that is presented in Figure 8, exhibit a high degree of roughness and sometimes oscillation which may be due the effect of interface zones of cement mortar and coarse aggregate that contribute sufficiently the shear stress of concrete. The minimum shear stress was found in prism made from Mix M3. This is may be the result of the use of larger aggregate particles in this concrete mix. The shear stress at the last loading increment for concrete made of Mix M2 is increased by 7.6 %when the tensile strength of the mortar is increased while changing the tensile strength of the mortar in other mixes increase the shear stress magnitudes at crack initiation. This shows the effect of the aggregate particles with the tensile strength of the mortar on the distribution of the shear stress in concrete as shown in Figure 8.

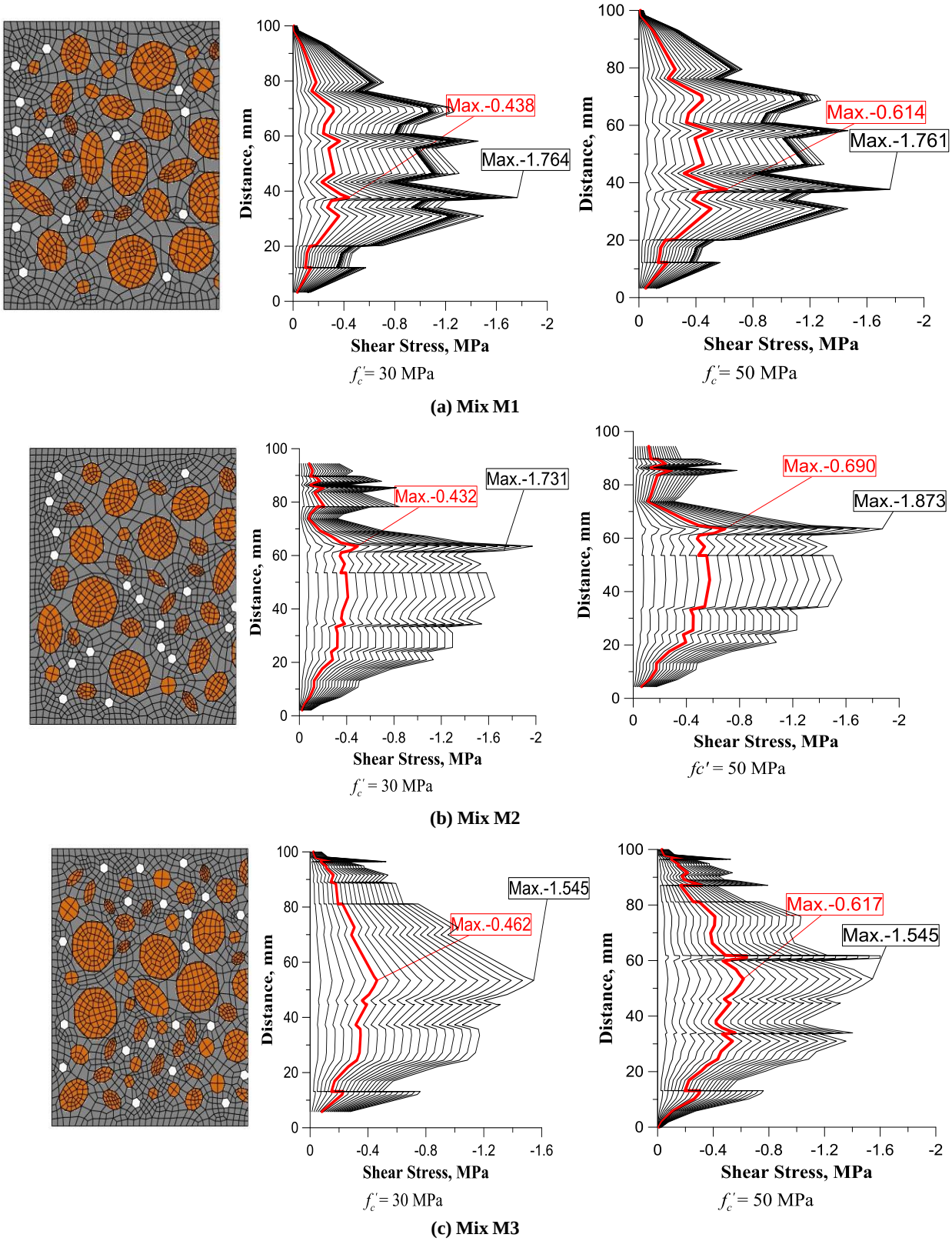

Figure 8. Effect of variation of coarse aggregate percentages on the shear stress distribution across prism section 84 mm from the left support at crack initiation and in the last loading increment

It is observed from Figure 9 that crack in plain concrete under flexural stresses will starts growing in about 20% of the total applied load, where P is the applied load, and Pf is the failure load. The crack will keep propagate in cement mortar until the crack path hits a stronger material such as coarse aggregate. The maximum crack depth of the three mixtures depends on the random distribution of the coarse aggregate particles.

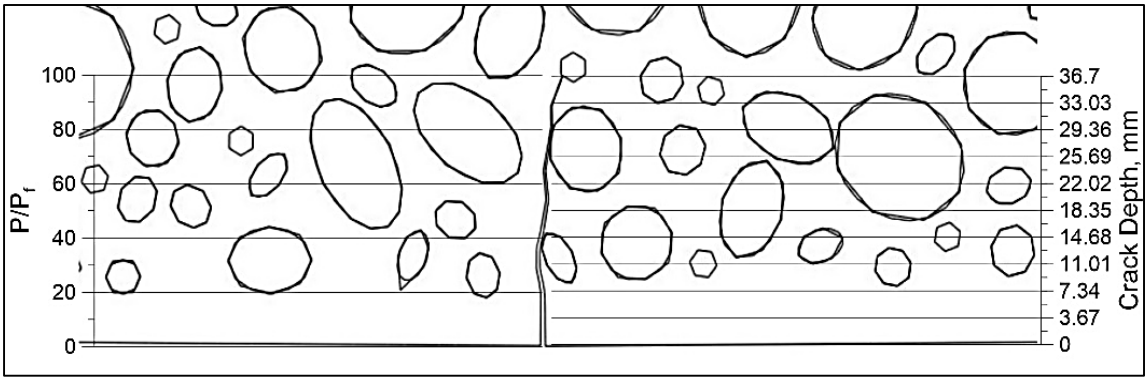

(a) Mix M1

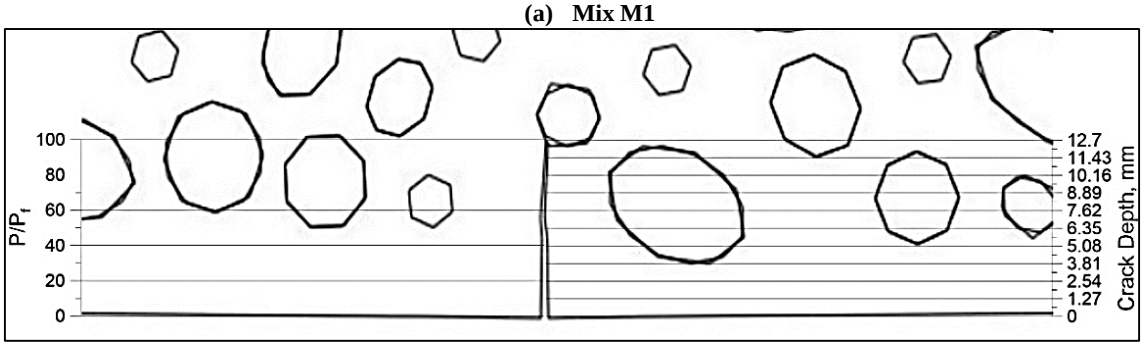

(b) Mix M2

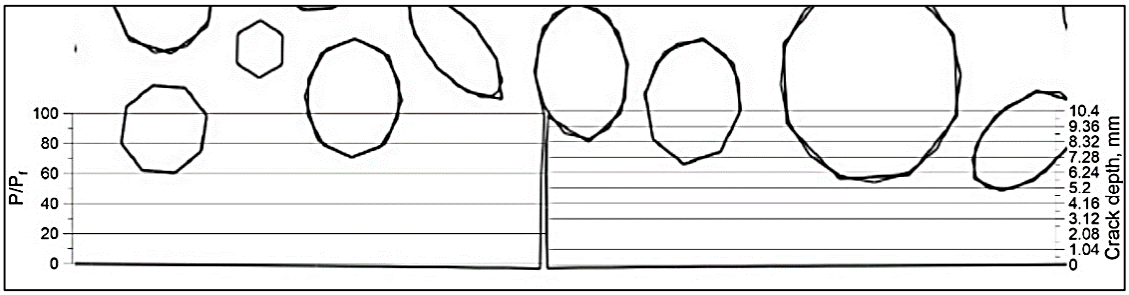

(c) Mix M3

Figure 9. Crack propagation due to the loading percentage of the total load for fc' = 30 MPa

8. Conclusion

Numerical models of concrete prisms in meso-scale two dimensional structure were conducted to be analyzed in this study. These models comprised of coarse aggregate, mortar, and air pores. Aggregate and pores were randomly distributed on the model section area. The shape of aggregate particles were elliptical with random sizes within the limit of coarse aggregate grading. Air pores were circular in shape and have the same diameter for all pores. The models were subjected to two point loading state, and the crack initiation and propagation were simulated using the Extended Finite Element Method (XFEM). The effect of aggregate grading and pores existing were investigated, and the following main conclusions were drawn:

- The bending stress and shear stress of the models were highly sensitive by the random microstructures. The size and distribution of aggregate particles are affecting on the maximum bending and shear stress, and the post-peak of the bending and shear stress are more effected and sensitive.
- Crack initiation and propagation have clear effect on the general behavior of concrete prisms, and the bending stress curves are falling to zero at crack location.
- The deflection was affected by the grading and particle size of the coarse aggregate. Maximum deflection was detected when the aggregate particles are smaller. While the bending stress was maximum when coarse aggregate

particles are bigger.

- The shear stress distribution was found to have a non-uniform oscillation trend across the beam section. This is due to the non-homogeneity of cement Mix. The importance of the meso-scale concrete analysis, may be seeked here.
- The pores size and position in the models have adverse effect on the concrete prisms strength. Consequently it cannot be neglected in the meso-scale analysis of concrete members.
- The crack propagation of the concrete is affected by the tensile strength of the mortar, however concrete of smaller maximum size of aggregate the tensile strength of the mortar affect the whole fracture process of concrete model.
- Plain concrete strength increased with the decreasing of aggregate particles and increasing of the tensile strength of the mortar.

9. References

[1] Grassl, Peter, David Grégoire, Laura Rojas Solano, and Gilles Pijaudier-Cabot. "Meso-Scale Modelling of the Size Effect on the Fracture Process Zone of Concrete." International Journal of Solids and Structures 49, no. 13 (June 2012): 1818–1827. doi:10.1016/j.ijsolstr.2012.03.023.

[2] Ren, W. Y., Z. J. Yang, and Phil Withers. "Meso-scale fracture modelling of concrete based on X-ray computed tomography images." In The 5th Asia-Pacific congress on computational mechanics (APCOM). Singapore. 2013.

[3] Lu, Yong, and Zhenguo Tu. "Mesoscale Modelling of Concrete for Static and Dynamic Response Analysis -Part 2: Numerical Investigations." Structural Engineering and Mechanics 37, no. 2 (January 25, 2011): 215–231. doi:10.12989/sem.2011.37.2.215.

[4] Wang, Xiaofeng, Zhenjun Yang, and Andrey P. Jivkov. "Monte Carlo simulations of mesoscale fracture of concrete with random aggregates and pores: a size effect study." Construction and Building Materials 80 (2015): 262-272.

[5] Wang, Xiaofeng, Mingzhong Zhang, and Andrey P. Jivkov. "Computational Technology for Analysis of 3D Meso-Structure Effects on Damage and Failure of Concrete." International Journal of Solids and Structures 80 (February 2016): 310–333. doi:10.1016/j.ijsolstr.2015.11.018.

[6] Mostafavi, M., N. Baimpas, E. Tarleton, R. C. Atwood, S. A. McDonald, A. M. Korsunsky, and T. J. Marrow. "Three-dimensional crack observation, quantification and simulation in a quasi-brittle material." Acta Materialia 61, no. 16 (2013): 6276-6289.

[7] Jivkov AP, Engelberg DL, Stein R, Petkovski M. Pore space and brittle damage evolution in concrete. Eng Fract Mech 2013;110:378–95.

[8] Yang, Z.J., X.T. Su, J.F. Chen, and G.H. Liu. "Monte Carlo Simulation of Complex Cohesive Fracture in Random Heterogeneous Quasi-Brittle Materials." International Journal of Solids and Structures 46, no. 17 (August 2009): 3222–3234. doi:10.1016/j.ijsolstr.2009.04.013.

[9] Leite, J.P.B., V. Slowik, and H. Mihashi. "Computer Simulation of Fracture Processes of Concrete Using Mesolevel Models of Lattice Structures." Cement and Concrete Research 34, no. 6 (June 2004): 1025–1033. doi:10.1016/j.cemconres.2003.11.011.

[10] Schlangen, E., and E.J. Garboczi. "Fracture Simulations of Concrete Using Lattice Models: Computational Aspects." Engineering Fracture Mechanics 57, no. 2–3 (May 1997): 319–332. doi:10.1016/s0013-7944(97)00010-6.

[11] Oliver, J. "A Consistent Characteristic Length for Smeared Cracking Models." International Journal for Numerical Methods in Engineering 28, no. 2 (February 1989): 461–474. doi:10.1002/nme.1620280214.

[12] Rots, Jan Gerrit. "Computational modeling of concrete fracture." PhD diss., Technische Hogeschool Delft, 1988.

[13] Bažant, Zdeněk P., and B. H. Oh. "Crack Band Theory for Fracture of Concrete." Matériaux et Constructions 16, no. 3 (May 1983): 155–177. doi:10.1007/bf02486267.

[14] Melenk, J.M., and I. Babuška. "The Partition of Unity Finite Element Method: Basic Theory and Applications." Computer Methods in Applied Mechanics and Engineering 139, no. 1–4 (December 1996): 289–314. doi:10.1016/s0045-7825(96)01087-0.

[15] Rabczuk, T., and T. Belytschko. "Cracking Particles: a Simplified Meshfree Method for Arbitrary Evolving Cracks." International Journal for Numerical Methods in Engineering 61, no. 13 (2004): 2316–2343. doi:10.1002/nme.1151.

[16] Unger, Jörg F., Stefan Eckardt, and Carsten Könke. "Modelling of cohesive crack growth in concrete structures with the extended finite element method." Computer Methods in Applied Mechanics and Engineering 196, no. 41-44 (2007): 4087-4100.

[17] Monteiro, A.B., A.R.V. Wolenski, F.B. Barros, R.L.S. Pitangueira, and S.S. Penna. "A Computational Framework for G/XFEM Material Nonlinear Analysis." Advances in Engineering Software 114 (December 2017): 380–393. doi:10.1016/j.advengsoft.2017.08.002.

[18] Huang, Yucheng, Yanhua Guan, Linbing Wang, Jian Zhou, Zhi Ge, and Yue Hou. "Characterization of Mortar Fracture Based on Three Point Bending Test and XFEM." International Journal of Pavement Research and Technology (September 2017). doi:10.1016/j.ijprt.2017.09.005.

[19] Du, Xiuli, Liu Jin, and Guowei Ma. "Numerical Modeling Tensile Failure Behavior of Concrete at Mesoscale Using Extended Finite Element Method." International Journal of Damage Mechanics 23, no. 7 (December 11, 2013): 872–898.

doi:10.1177/1056789513516028.

[20] López, Carlos M., Ignacio Carol, and Antonio Aguado. "Meso-Structural Study of Concrete Fracture Using Interface Elements. I: Numerical Model and Tensile Behavior." Materials and Structures 41, no. 3 (November 6, 2007): 583–599. doi:10.1617/s11527-007-9314-1.

[21] ACI 318-95 (1995), "Building Code Requirements for Structural Concrete", American Concrete Institution, United State.

[22] Callister Jr, William D. "Materials Science and Engineering - An Introduction (5th Ed.)." Anti-Corrosion Methods and Materials 47, no. 1 (February 2000). doi:10.1108/acmm.2000.12847aae.001.

[23] Bazant, Z. P. (Ed.). (1992). Fracture Mechanics of Concrete Structures: Proceedings of the First International Conference on Fracture Mechanics of Concrete Structures (FraMCoS1), held at Beaver Run Resort, Breckenridge, Colorado, USA, 1-5 June 1992 (Vol. 1). CRC Press.

[24] ASTM C33 / C33M-16, Standard Specification for Concrete Aggregates, ASTM International, West Conshohocken, PA, 2016, www.astm.org, doi: 10.1520/C0033_C0033M-16.

[25] Shahbazi, Siamak, and Iraj Rasoolan. "Meso-Scale Finite Element Modeling of Non-Homogeneous Three-Phase Concrete." Case Studies in Construction Materials 6 (June 2017): 29–42. doi:10.1016/j.cscm.2016.10.002.

[26] Khoei A. R. "Extended Finite Element Method Theory and Application" (December 18, 2014), doi: 10.1002/9781118869673.

[27] Asferg, J.L., Poulsen, P. N. and Nielsen, L. O., "A direct XFEM formulation for modeling of cohesive crack growth in concrete", Computer and Concrete 4(2), (April 25 2007): 83-100. doi: 10.12989/cac.2007.4.2.083.

[28] Osher, Stanley, and James A Sethian. "Fronts Propagating with Curvature-Dependent Speed: Algorithms Based on Hamilton-Jacobi Formulations." Journal of Computational Physics 79, no. 1 (November 1988): 12–49. doi:10.1016/0021-9991(88)90002-2.

[29] Sukumar, N., D.L. Chopp, N. Moës, and T. Belytschko. "Modeling Holes and Inclusions by Level Sets in the Extended Finite-Element Method." Computer Methods in Applied Mechanics and Engineering 190, no. 46–47 (September 2001): 6183–6200. doi:10.1016/s0045-7825(01)00215-8.

[30] Erdogan, F., and G. C. Sih. "On the Crack Extension in Plates under Plane Loading and Transverse Shear." Journal of Basic Engineering 85, no. 4 (1963): 519. doi:10.1115/1.3656897.